Circulation Research

ORIGINAL RESEARCH

Transcription Factor 21 Regulates Cardiac Myofibroblast Formation and Fibrosis

Anne Katrine Z. Johansen, Rajesh K. Kasam, Ronald J. Vagnozzi, Suh-Chin J. Lin, Jose Gomez-Arroyo, Adenike Shittu, Stephanie L.K. Bowers, Yasuhide Kuwabara, Kelly M. Grimes, Kathrynne Warrick, Michelle A. Sargent, Tanya A. Baldwin, Susan E. Quaggin, Artem Barski, Jeffery D. Molkentin

BACKGROUND: TCF21 (transcription factor 21) is a bHLH (basic helix-loop-helix) protein required for the developmental specification of cardiac fibroblasts (CFs) from epicardial progenitor cells that surround the embryonic heart. In the adult heart, TCF21 is expressed in tissue-resident fibroblasts and is downregulated in response to injury or stimuli leading to myofibroblast differentiation. These findings led to the hypothesis that TCF21 regulates fibroblast differentiation in the adult mammalian heart to affect fibrosis.

METHODS: Tamoxifen-inducible Cre genetic mouse models were used to permit either *Tcf21* gene deletion or its enforced expression in adult CFs. Histological and echocardiographic analyses were used, as well as transcriptomic analysis to determine the consequences of TCF21 gain-of-function and loss-of-function in vivo. Genomic *Tcf21* occupancy was identified by chromatin immunoprecipitation and sequencing in CFs. Myocardial infarction and AngII (angiotensin II)/phenylephrine served as models of cardiac fibrosis.

RESULTS: Acute and long-term deletion of *Tcf21* in CFs of the adult mouse heart does not alter fibroblast numbers, myofibroblast differentiation, or fibrosis. Fibroblast-specific *Tcf21* gene–deleted mice demonstrate no significant alterations in cardiac function or scar formation in response to cardiac injury compared with control mice. In contrast, enforced expression of TCF21 in CFs inhibits myofibroblast differentiation and significantly reduces cardiac fibrosis and hypertrophy in response to 1 week of Ang II/phenylephrine infusion. Mechanistically, sustained TCF21 expression prevents the induction of genes associated with fibrosis and ECM (extracellular matrix) organization.

CONCLUSIONS: TCF21 expression is not required to maintain the cell state of CFs in the adult heart. However, preventing the normal downregulation of TCF21 expression with injury reduces myofibroblast formation, cardiac fibrosis, and the acute cardiac hypertrophic response following 1 week of Ang II/phenylephrine stimulation.

GRAPHIC ABSTRACT: A graphic abstract is available for this article.

Key Words: cardiomyopathies ■ extracellular matrix ■ fibroblasts ■ fibrosis ■ myofibroblasts

Meet the First Author, see p 2

TCF21 (transcription factor 21) is a class II bHLH (basic helix-loop-helix) protein that is essential for the fate specification of epicardial progenitor cells to cardiac fibroblasts (CFs) during embryonic heart development.[1] bHLH proteins are a large family of dimeric transcription factors that have essential roles in cell specification, differentiation, and development. Class I bHLH transcription factors (also known as E proteins) are ubiquitously expressed, whereas class II bHLH proteins are cell-type specific but require class I proteins to form dimers and exert their function. TCF21 forms a heterodimer with other bHLH proteins including E12 to bind the E-box consensus DNA sequence 5'CANNTG.[2] TCF21 is expressed in adult CFs and is downregulated in response to stimuli that promote fibroblast activation and differentiation to a smooth muscle-like cell, the

Correspondence to: Jeffery D. Molkentin, PhD, Department of Pediatrics, 3333 Burnet Ave, Cincinnati Children's Hospital Medical Center, Cincinnati, OH 45229. Email jeff.molkentin@cchmc.org

Supplemental Material is available at https://www.ahajournals.org/doi/suppl/10.1161/CIRCRESAHA.124.325527.
For Sources of Funding and Disclosures, see page 56.

Circulation Research is available at www.ahajournals.org/journal/res

Novelty and Significance

What Is Known?

- TCF21 (transcription factor 21) is required for the fate specification and development of the cardiac fibroblast lineage.
- TCF21 expression is downregulated in response to insults that promote cardiac fibroblast activation, differentiation, and the induction of fibrosis.

What New Information Does This Article Contribute?

- Deletion of endogenous *Tcf21* in the mouse did not alter disease-induced cardiac fibrosis.
- The downregulation of TCF21 is necessary for the development of cardiac fibrosis.

TCF21 is a basic helix-loop-helix transcription factor that plays essential roles in fate specification and differentiation in different cell types. In the heart, TCF21 is required for the formation of the cardiac fibroblast lineage and remains expressed in adult quiescent fibroblasts. In response to injury or disease, fibroblasts convert into fibrosis-producing myofibroblasts, which is associated with downregulation of TCF21 expression in previous studies. This led to the hypothesis that TCF21 regulates fibroblast differentiation in the adult mammalian heart to affect fibrosis with disease stimulation. Using genetic mouse models with loss-of-function and gain-of-function for TCF21, we demonstrate that only increased and sustained expression of TCF21 inhibits the formation of myofibroblasts and stimulus-induced fibrosis. By performing mRNA sequencing and chromatin immunoprecipitation, we show that TCF21 regulates the fibrotic response, in part, by also binding within key genes associated with myofibroblast function. In summary, these studies demonstrate that while loss of *Tcf21* has little discernible effect on fibroblast biology in the heart, preventing its downregulation can inhibit fibroblast differentiation to the myofibroblast and the fibrotic response with injury.

Nonstandard Abbreviations and Acronyms

Ang II	angiotensin II
bHLH	basic helix-loop-helix
CF	cardiac fibroblast
COMP	cartilage oligomeric matrix protein
ECM	extracellular matrix
fl	flanking loxP sites for Cre recombinase
LV	left ventricle
MCM	MerCreMer
MI	myocardial infarction
POSTN	periostin
qRT-PCR	quantitative real-time PCR
Rosa26-eGFP	Rosa26-loxP-STOP-loxP-enhanced green fluorescent protein
TCF21	transcription factor 21
αSMA	smooth muscle α-actin

myofibroblast.[3–5] In human coronary artery smooth muscle cells, the knockdown of *Tcf21* induces the expression of smooth muscle genes, including *Acta2* and *Tagln*,[6] which are also associated with the myofibroblast.[7,8] These data suggest that TCF21 can function as a gene repressor[6,9] to maintain the resting fibroblast state and that loss of TCF21 might impact fibroblast identity and activity in vivo, with a potential impact on fibrosis development.

In humans, ischemic, hypertensive, or genetic cardiomyopathies are all characterized by different degrees of interstitial and replacement fibrosis,[10] which is associated with worse clinical outcomes and increased mortality.[11] Fibroblasts regulate cardiac tissue architecture by synthesis of ECM (extracellular matrix) proteins, growth factors, and cytokines that collectively impact the mechanical properties of the heart and the cardiomyocyte hypertrophic response.[12] Studies in mice have demonstrated that altering fibroblast activation and differentiation can benefit cardiac function in models of ischemic and hypertensive cardiomyopathy.[13–15]

Here, we demonstrate that TCF21 is an important effector of fibroblast conversion to myofibroblasts using a conditional gene deletion model and a spatiotemporal

model of enforced TCF21 expression in vivo. While the loss of TCF21 from adult CFs did not alter their function or ability to differentiate into myofibroblasts, sustained TCF21 expression in adult fibroblasts inhibited myofibroblast formation, ECM deposition, and the cardiac hypertrophic response after injury. Thus, while TCF21 is not required to maintain adult quiescent fibroblast activity, downregulation of TCF21 in the CF is necessary to form myofibroblasts and drive cardiac fibrosis.

METHODS

Data Availability

Bulk RNA, single-cell, and chromatin immunoprecipitation sequencing data sets have been deposited to the Gene Expression Omnibus as annotated in the Major Resources Table.

All experiments were performed in accordance with the guidelines and approval by the Institutional Animal Care and Use Committee at Cincinnati Children's Hospital. A detailed description of all methods and materials utilized in the study can be found in the Supplemental Methods. A list of all reagents and their catalog numbers can be found in the Major Resources Table.

RESULTS

Genetic Loss of *Tcf21* Does Not Promote Fibroblast Differentiation to Myofibroblasts

To assess if loss of TCF21 affects the differentiation of fibroblasts to myofibroblasts, the previously described *Tcf21* targeted allele with exon 1 flanked (fl) by two loxP (locus of crossover in P1) sites[16] targeted allele was used in conjunction with tamoxifen-inducible fibroblast Cre expressing alleles. First, to validate the targeted allele, $Tcf21^{fl/fl}$ mice were crossed with transgenic mice ubiquitously expressing Cre under the transcriptional control of a cytomegalovirus promoter (cytomegalovirus-Cre; Figure S1A). This generated a peripartum lethal phenotype as previously described in germline-deleted *Tcf21* mice.[1,17,18] $Tcf21^{fl/fl}$: cytomegalovirus-Cre mice were harvested at embryonic (E) day 18.5, and gross morphometric analysis revealed the expected hypoplastic lungs and kidneys, grossly abnormal heart, and the absence of a spleen, which verifies the integrity of the loxP targeted allele. $Tcf21^{fl/fl}$ mice were used as controls (Figure S1B and S1C). Next, CFs were isolated from adult $Tcf21^{fl/fl}$ mice and infected with an adenovirus-encoding Cre recombinase to induce genetic recombination in vitro versus an adenovirus-encoding beta-galactosidase as a control. Cells harvested 3 days after infection exhibited loss of *Tcf21* at the mRNA and protein levels (Figure 1A and 1B). Immunoblotting was performed for αSMA (smooth muscle α-actin, *Acta2* gene; Figure 1B), and quantitative real-time PCR (qRT-PCR) was used to assess *Acta2* and *Tagln* (SM22 protein) mRNA expression, which revealed no statistically significant differences between Cre recombinase or beta-galactosidase–infected cells (Figure 1C).

To study the function of TCF21 in vivo, $Tcf21^{fl/fl}$ mice were crossed with *Tcf21-MerCreMer* ($Tcf21^{MCM}$) mice to permit genetic recombination and ablation of *Tcf21* in all TCF21-expressing cells upon exposure to tamoxifen (Figure 1D). $Tcf21^{MCM}$ mice were used as controls, which are heterozygous for *Tcf21* due to the insertion of the MCM (MerCreMer) cDNA within that locus.[19] $Tcf21^{MCM}$ mice display wild-type levels of TCF21 protein expression (data not shown). All mice had a genetic reporter consisting of 1 *Rosa26-eGFP* (*Rosa26*-loxP-STOP-loxP-enhanced green fluorescent protein) allele, which tracks fibroblasts with recombination activity due to $Tcf21^{MCM}$. First, to examine *Tcf21* deletion, eGFP+ CFs were isolated from the hearts of adult mice using FAC (fluorescence-activated cell) sorting 2 weeks after the first tamoxifen injection (Figure 1D). qRT-PCR analysis confirmed the deletion of *Tcf21* at the transcript level (Figure 1E). Immunofluorescence analysis of the eGFP+ CFs in $Tcf21^{fl/MCM}$ hearts demonstrated a lack of expression of the myofibroblast markers, αSMA (*Acta2* gene; Figure 1F, in red), and SM22 (transgelin, *Tagln* gene; Figure 1G, in red), suggesting that *Tcf21* ablation alone is insufficient to promote fibroblast differentiation into myofibroblasts in vivo after 2 weeks. As expected, αSMA and SM22 protein expressions were observed in the vessels of $Tcf21^{fl/MCM}$ and $Tcf21^{MCM}$ control mice due to the presence of smooth muscle cells (Figures 1F and 1G, white arrows).

To further examine the function of *Tcf21*, bulk RNA transcriptional profiling of FAC-sorted eGFP+ CFs isolated 2 weeks after the first tamoxifen injection was performed. This identified 209 downregulated (log_2-fold change [FC] >−1; false discovery rate <0.1) and 179 upregulated genes (log_2-FC >1; false discovery rate <0.1) in $Tcf21^{fl/MCM}$ versus $Tcf21^{MCM}$ control eGFP+ CFs (Figure 1H; Table S1). Analysis of *Tcf21* normalized transcript counts confirmed downregulation by the loxP gene deletion strategy (Figure 1I). Gene ontology analysis of the upregulated genes showed sparingly few biological process pathways including cell adhesion (GO:0007155), positive regulation of angiogenesis (GO:0045766), positive regulation of chondrocyte proliferation (GO:1902732), and neutrophil chemotaxis (GO:0030593; Table S1). Of note, no significant differences were detected for signature myofibroblast genes, including *Postn*, *Acta2*, *Cnn1*, *Col1a1*, or *Col1a2*. Manual profiling of the upregulated genes identified only a small subset of genes associated with fibroblast activation and differentiation (Figure 1J). Gene ontology analysis of downregulated genes failed to detect a substantial number of pathways, with only 4 genes contributing to most of the pathways detected (Table S1).

To determine the long-term effect of *Tcf21* deletion on fibroblast differentiation, fibrosis, and cardiac function,

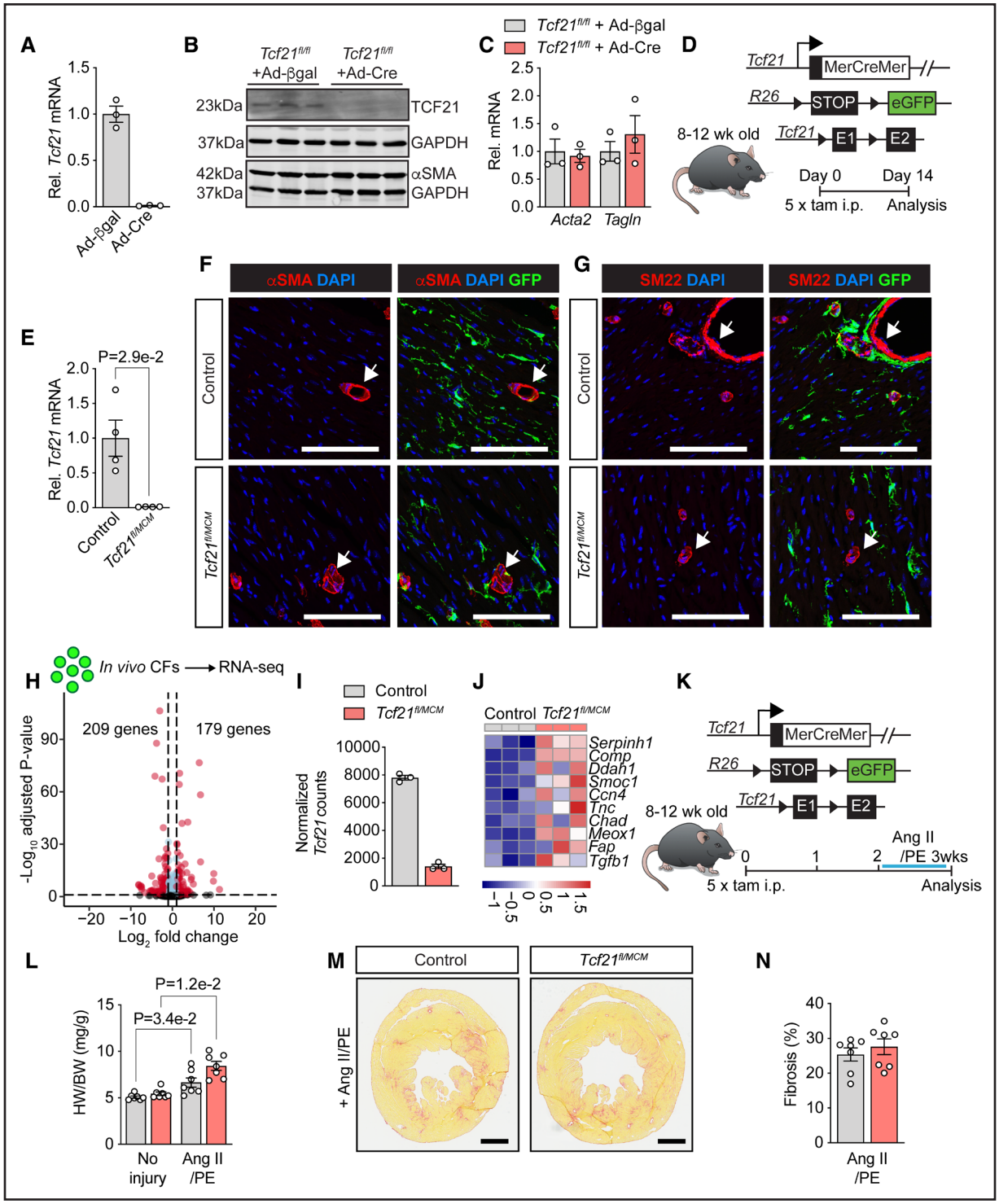

Figure 1. Genetic loss of *Tcf21* (transcription factor 21) in adult cardiac fibroblasts does not promote myofibroblast differentiation.

A, Quantitative real-time PCR (qRT-PCR) analysis of *Tcf21* mRNA and (**B**) immunoblot analysis of TCF21 and αSMA (smooth muscle α-actin) protein in cultured adult murine cardiac fibroblasts (CFs) from *Tcf21*$^{fl/fl}$ mice infected with Ad-βgal (adenovirus-encoding beta-galactosidase) or Ad-Cre (adenovirus-encoding Cre recombinase). Fifty micrograms of protein were loaded, and GAPDH was used as a loading/normalization control. **C**, qRT-PCR analysis of *Acta2* and *Tagln* mRNA from the indicated samples in cultured adult murine CFs from the indicated genotypes of mice with the 2 adenoviral infections in culture. **D**, Schematic of the genetically modified mouse alleles used and temporal experimental outline. This cross also contained the *Rosa26-eGFP* (enhanced green fluorescent protein) conditional reporter allele to show fluorescence within recombined fibroblasts. Tamoxifen (tam) was administered to 8- to 12-week-old mice for 5 consecutive days by intraperitoneal injection (i.p.) and harvested 14 days later. **E**, qRT-PCR analysis of *Tcf21* mRNA expression from eGFP+ sorted CFs from *Tcf21*$^{fl/MCM}$ mice vs *Tcf21*^{MCM} controls. **F** and **G**, Immunofluorescence microscopy analysis of heart histological sections for the myofibroblast (*Continued*)

the hearts of *Tcf21*$^{fl/MCM}$ and *Tcf21*^{MCM} control mice were analyzed 15 weeks after tamoxifen injection. Immunofluorescence analysis of the eGFP+ CFs in *Tcf21*$^{fl/MCM}$ hearts demonstrated a lack of expression of the myofibroblast markers, αSMA or SM22 (Figure S2A and S2B). Sirius red–stained histological sections revealed no indication of cardiac fibrosis (Figure S2C and S2D). In addition, the loss of *Tcf21* after 15 weeks had no statistically significant differences in overall cardiac structure and function as determined by heart weight/body weight ratios (Figure S2E), left ventricular (LV) wall thickness (Figure S2F), LV fractional shortening (Figure S2G), or LV internal diameter (Figure S2H).

To further validate these findings, *Tcf21*$^{fl/fl}$ mice were crossed with a different fibroblast-selective CreERT2 allele driven by the *Pdgfra* (platelet-derived growth factor receptor, alpha polypeptide) gene (*Pdgfra-CreERT2*),[20] and analyzed 6 weeks later (Figure S2I). *Pdgfra* is a mesenchymal marker expressed by most CFs and has been reported to target 30% more fibroblasts than *Tcf21*^{MCM}.[21–23] *Pdgfra*-driven deletion of *Tcf21* after 6 weeks had no statistically significant effects on cardiac structure and function, except for a slightly greater LV wall thickness as assessed by echocardiography (Figure S2J through S2M). Taken together, these data demonstrate no statistically different effects due to deletion of *Tcf21* from CFs in the adult mouse heart on fibroblast activation and cardiac structure/function.

Genetic Loss of *Tcf21* Does Not Alter Fibroblast Numbers in the Heart

It has been previously shown that the overexpression of *TCF21* in human coronary arterial smooth muscle cells induced cell proliferation.[6] In contrast, in certain cancer cell types, TCF21 can inhibit cell proliferation and promote apoptosis.[24] To determine whether CF quantity is affected by the loss of *Tcf21*, fibroblasts from *Tcf21*$^{fl/MCM}$ and *Tcf21*^{MCM} control mice were quantified by flow cytometry 15 weeks after tamoxifen-induced genetic recombination. No statistically significant differences in the number of eGFP+ CFs within the LV were found between the 2 groups (Figure S3A and S3B). Although transcriptional profiling identified ontological associations with cell adhesion and angiogenesis, quantification of the total number of leukocytes (CD45) and endothelial cells (CD31) by flow cytometry was not statistically different in *Tcf21*$^{fl/MCM}$ versus *Tcf21*^{MCM} control hearts (Figure S3C and S3D). A similar inert profile was observed when *Pdgfra-CreERT2* was used to delete *Tcf21* in CFs (Figure S3E through S3G).

Genetic Loss of *Tcf21* Does Not Impact Fibrosis After Angiotensin II/Phenylephrine-Induced Cardiac Injury

To determine whether the loss of TCF21 in fibroblasts before a cardiac injury affects the development of fibrosis, tamoxifen-treated *Tcf21*$^{fl/MCM}$ and *Tcf21*^{MCM} or *Tcf21*$^{fl/fl}$ control mice were exposed to a continuous infusion of Ang II (angiotensin II)/phenylephrine for 1 week (Figure 1K). Cardiac hypertrophy was present in both cohorts of mice as determined by heart weight/body weight ratios (Figure 1L). To assess the extent of cardiac fibrosis, multiple nonsequential (1 mm apart) heart histological sections (at least 4 per mouse) were analyzed for collagen deposition using Sirius red staining. No statistically significant differences in the induction of cardiac fibrosis were detected when comparing hearts from *Tcf21*$^{fl/MCM}$ with either *Tcf21*^{MCM} control mice (Figure 1M and 1N) or *Tcf21*$^{fl/fl}$ control mice (data not shown). To further define the effect of the genetic loss of *Tcf21* on CFs after Ang II/phenylephrine exposure, bulk RNA transcriptional profiling was performed on FAC-sorted eGFP+ CFs. Principle component analysis demonstrated unique occupancies within the transcriptional space between the groups (Figure S4A). Normalized transcript counts confirmed reduced expression of *Tcf21* (Figure S4B). Differential gene expression analysis identified 200 downregulated ($\log_2$-FC >—1; false discovery rate <0.1) and 122 upregulated genes ($\log_2$-FC >1; false discovery rate <0.1) in *Tcf21*$^{fl/MCM}$ versus *Tcf21*^{MCM} control eGFP+ CFs (Figure S4C; Table S2). Only a few genes were associated with ontology pathways of either upregulated or downregulated genes in *Tcf21*$^{fl/MCM}$ fibroblasts compared with *Tcf21*^{MCM} control

Figure 1 Continued. markers (**F**) αSMA and (**G**) transgelin (SM22) as denoted by red fluorescence. eGFP (green) shows the presence of the recombined fibroblasts due to the *Rosa26-eGFP* reporter allele, and nuclei are shown in blue with 4′,6-diamidino-2-phenylindole (DAPI) staining. The arrows show areas of cardiac vessels as controls that are positive for smooth muscle gene expression with αSMA and SM22. Scale bars, 50 μm. **H**, Volcano plot of differentially expressed mRNAs as detected by bulk transcriptomic sequencing from fluorescence-activated cell (FAC) sorting of eGFP+ CFs from *Tcf21*$^{fl/MCM}$ mice vs *Tcf21*^{MCM} controls. **I**, Normalized *Tcf21* transcript counts from these samples in **H**. **J**, Heatmap of Z-score normalized read counts of manually selected fibrosis-associated genes in CFs of *Tcf21*$^{fl/MCM}$ vs *Tcf21*^{MCM} control mice. **K**, Schematic of the genetically modified mouse alleles used and experimental outline. Tam was administered to 8- to 12-week-old mice for 5 consecutive days by i.p. injection followed by 1 week of Ang II (angiotensin II)/phenylephrine (PE) stimulation before analysis. **L**, Heart weight to body weight ratio (HW/BW). **M**, Representative whole heart histological images stained with Sirius red for collagen deposition from the 2 groups of mice shown. Scale bars, 1 mm. **N**, Quantification of percentage area of tissue fibrosis as shown in **M**. All data shown are mean±SEM. Samples were analyzed by a Kolmogorov-Smirnov test (exact *P* values are shown; **E** and **N**) or a Scheirer-Ray-Hare test with a Dunn post hoc test and the Benjamini Hochberg method for multiple test correction (exact adjusted *P* values are shown; **L**). For cell culture experiments, each n value is an independent pool of CFs obtained from 1 male and 1 female mouse heart. All other data points in the graphs represent biological replicates. SM22 indicates the protein product from the *Tagln* gene.

fibroblasts after 1 week of Ang II/phenylephrine (Table S2). Taken together, these data suggest that the loss of TCF21 before the induction of fibrosis with Ang II/phenylephrine does not alter the fibroblast transcriptome, nor impact the fibrotic response.

Cardiac Single-Cell RNA Transcriptomic Analysis of Interstitial Cells Identifies Altered Cell Compositions

Single-cell RNA sequencing was used to further examine the potential effect of *Tcf21* deletion on fibroblast cell states and neighboring interstitial cells within the heart. Single-cell RNA sequencing was performed on FAC-sorted cells from the LV of tamoxifen-treated uninjured *Tcf21*$^{fl/MCM}$ and *Tcf21*^{MCM} control mice and after an acute (3-day) myocardial infarction (MI) injury (Figure 2A). MI is known to activate CFs and lead to immune cell infiltration and expansion. After quality control, a total of 7379 *Tcf21*^{MCM} and 8184 *Tcf21*$^{fl/MCM}$ cells from uninjured hearts and 4964 *Tcf21*^{MCM} and 5391 *Tcf21*$^{fl/MCM}$ cells from the infarcted and border-zone regions of MI hearts were used for downstream analysis. Figure 2B shows a projection of cells analyzed after data integration, normalization, and clustering. Thirteen cardiac cell subpopulations were identified using data from a pool of 4 male mice per condition (Figure 2B and 2C). These cell populations included B cells (*Cd79a*, *Cd79b*, and *Ms4a1*), dendritic cells (*H2-ab1* and *Cd74*), endothelial cells I (*Fabp4*, *Kdr*, and *Cdh5*), endothelial cells II (*Eng* and *Epas1*), fibroblasts (*Dcn*, *Dpt*, *Col1a1*, *Col1a2*, and *Pdgfra*), macrophages (*Lyz2*, *Cd68*, and *Ccl2*), myofibroblasts (*Acta2*, *Tnc*, *Col1a1*, *Col1a2*, *Postn*, and *Tagln*), natural killer cells (*Ccl5*, *Ms4a4b*, and *Nkg7*), neutrophils (*S100a8* and *S100a9*), Schwann cells (*Plp1* and *Kcna1*), smooth muscle cells (*Rgs5*, *Vtn*, *Tagln*, and *Myh11*), and tissue-resident macrophages (*Cx3cr1*, *Lyve1*, and *Cd74*; Figure 2B and 2C). Visualization of cluster contributions demonstrated similar cell ratios between *Tcf21*^{MCM} controls and *Tcf21*$^{fl/MCM}$ mice although minor differences were observed (Figure 2C). Analysis of only eGFP expressing CFs (>2 counts) in the uninjured heart showed no detectable differences in fibroblast cell states (Figure 2D), further suggesting that the loss of *Tcf21* does not impact differentiation.

Visualizations of cell ratios between the hearts of *Tcf21*$^{fl/MCM}$ and *Tcf21*^{MCM} control mice demonstrated more neutrophils in *Tcf21*$^{fl/MCM}$ mice (Figure 2C). Consistent with these findings, gene ontology analysis from bulk RNA data sets also identified a small subset of genes associated with neutrophil chemotaxis, including *Cxcl5* (Figure S5A). Given that cell populations detected by single-cell RNA sequencing do not directly reflect changes in total cell content, LV tissue homogenates of *Tcf21*$^{fl/MCM}$ and *Pdgfra-CreERT2:Tcf21*$^{fl/fl}$ mice were analyzed by flow cytometry 4 weeks after tamoxifen injection for the presence of neutrophils (Figure S5B and S5C). *Tcf21*^{MCM} *and Pdgfra-CreERT2* mice were used as controls, respectively. Gating consisted of doublet exclusion with specific cell-surface markers for the detection of neutrophils and monocytes (Figure S5D). No statistically significant differences in Ly6C low- or high-expressing monocytes were observed between control and mice lacking *Tcf21* with either the *Tcf21*^{MCM} or the *Pdgfra-CreERT2* allele used to ablate the loxP targeted allele (Figure S5E, S5F, S5H, and S5I). However, neutrophil content was slightly but significantly elevated in the hearts of both *Tcf21*$^{fl/MCM}$ and *Pdgfra-CreERT2:Tcf21*$^{fl/fl}$ mice (Figure S5G through S5J).

The Genetic Loss of *Tcf21* Does Not Affect Cardiac Remodeling or Function After MI

In response to MI, immune cells (neutrophils, dendritic cells, bone marrow-derived macrophages, and natural killer cells) and myofibroblasts predominated the captured cell populations by single-cell RNA sequencing (Figure 2C). Fewer endothelial cells, tissue-resident fibroblasts, and macrophages were captured, which is consistent with previous analysis after MI.[25] Similar cell compositions between the hearts of controls and *Tcf21*$^{fl/MCM}$ mice were observed after MI although there were relatively fewer macrophages in the hearts of *Tcf21*$^{fl/MCM}$ mice compared with *Tcf21*^{MCM} hearts (Figure 2C).

To determine whether the genetic loss of *Tcf21* in fibroblasts alters cardiac remodeling in response to chronic ischemic injury, a separate cohort of tamoxifen-treated *Tcf21*$^{fl/MCM}$ and *Tcf21*^{MCM} control mice was studied 2 weeks after MI (Figure 2E). Deletion of *Tcf21* did not significantly change cardiac hypertrophy after 2 weeks of MI injury as determined by heart weight/body weight ratio measurement between *Tcf21*$^{fl/MCM}$ and *Tcf21*^{MCM} control mice (Figure 2F). Similarly, the MI-induced changes in LV wall thickness (Figure 2G) and LV ejection fraction (Figure 2H) were not statistically different when comparing *Tcf21*$^{fl/MCM}$ and *Tcf21*^{MCM} control mice. However, statistically, only *Tcf21*^{MCM} control mice had the expected reduction in LV ejection fraction, and only *Tcf21*$^{fl/MCM}$ had a reduction in LV wall thickness in response to MI. Compared with *Tcf21*^{MCM} control mice, genetic loss of *Tcf21* did not affect the induction of LV dilation induced by MI (Figure 2I). In addition, the degree and extent of fibrosis were not statistically different between the groups 2 weeks after MI (Figure 2J and 2K). Taken together, these findings suggest that deletion of *Tcf21* in adult CFs does not significantly alter cardiac remodeling or fibrosis in response to 2 weeks of chronic ischemia.

Generation and Validation of a Mouse Model With Enforced TCF21 Expression in CFs

TCF21 expression is downregulated in activated fibroblasts that differentiate into myofibroblasts,[3–5] suggesting

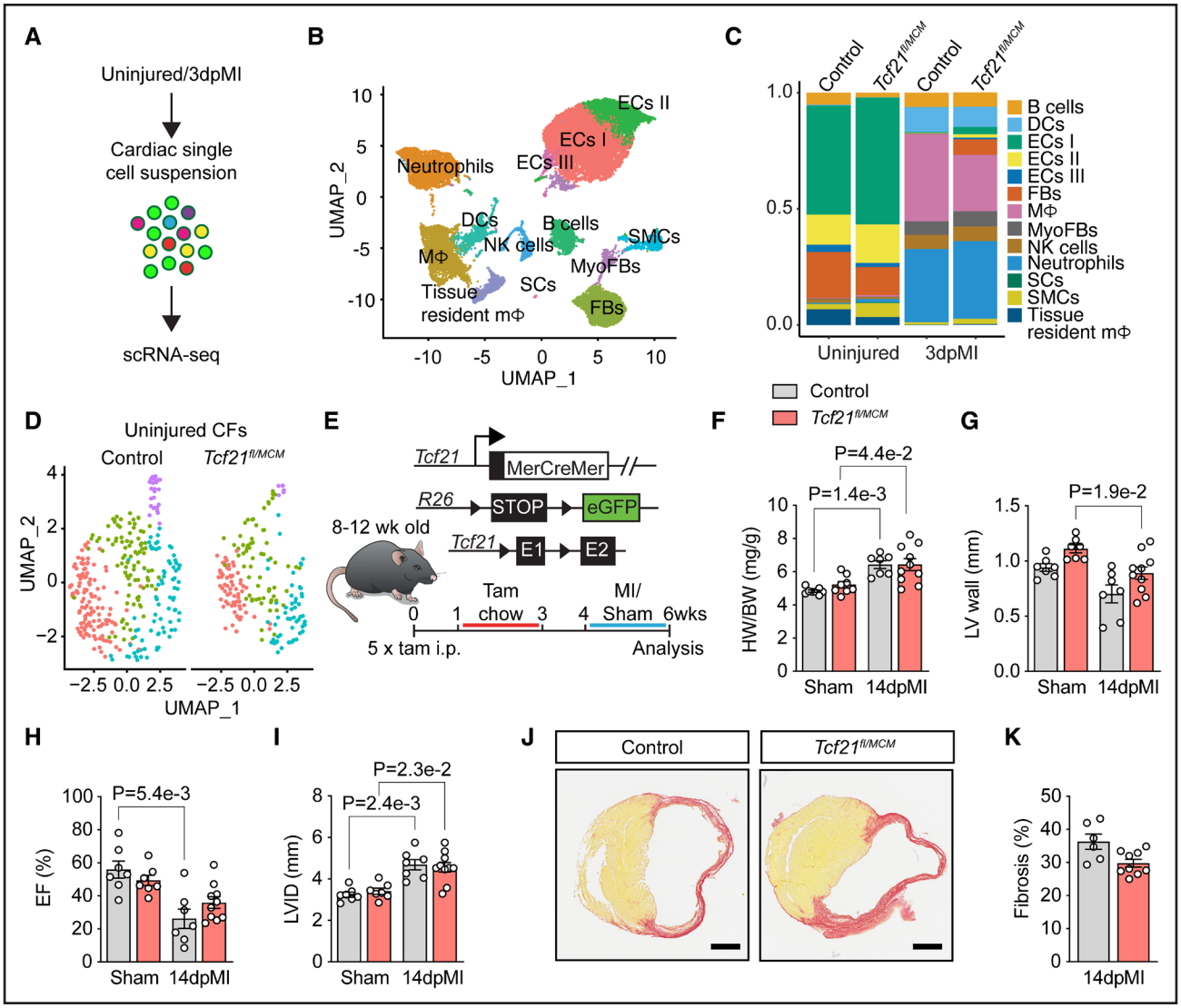

Figure 2. Loss of *Tcf21* does not affect cardiac function or fibrosis after myocardial infarction (MI).
A, Schematic of experimental outline for single-cell RNA sequencing (scRNA-seq) analysis from isolated cardiac interstitial cells from uninjured hearts and 3 days post-MI (3dpMI) from *Tcf21*$^{fl/MCM}$ mice and *Tcf21*^{MCM} controls. **B**, Uniform manifold approximation and projection (UMAP) of all single cells that passed quality control filtering from hearts of the groups discussed in **A**. **C**, DittoPlot of the cardiac cell populations in the groups of mice shown; controls were *Tcf21*^{MCM} mice. **D**, UMAP of reclustered uninjured eGFP (enhanced green fluorescent protein)+ (>2 counts) fibroblasts (FBs) from hearts of the 2 groups of mice shown. **E**, Schematic of the genetically modified mouse alleles used and temporal experimental outline. Tamoxifen (tam) was administered to 8- to 12-week-old mice for 5 consecutive days by intraperitoneal injection (i.p.) followed by 1 week of tam chow. One week later, mice were subjected to either sham or MI surgery before harvesting 14 days post-MI (14dpMI) for analysis of (**F**) heart weight to body weight (HW/BW) ratio and (**G**) echocardiographic analysis of left ventricular (LV) wall thickness in diastole, (**H**) ejection fraction (EF; %), and (**I**) LV internal chamber diameter in diastole (LVID). **J**, Representative whole heart histological images stained with Sirius red for collagen deposition from the 2 groups of mice shown. Scale bar, 1 mm. **K**, Quantification of percentage area of tissue fibrosis in *Tcf21*$^{fl/MCM}$ mice vs *Tcf21*^{MCM} controls as shown in **J**. All data shown are mean±SEM. Samples were analyzed by a Scheirer-Ray-Hare test with a Dunn post hoc test and the Benjamini Hochberg method for multiple test correction (exact adjusted *P* values are shown; **F**–**I** and **K**). All data points in graphs represent biological replicates. CF indicates cardiac fibroblasts; DC, dendritic cell; EC, endothelial cell; MΦ, macrophages; NK, natural killer; SC, Schwann cell; and SMC, smooth muscle cell.

that deleting this gene in fibroblasts before the induction of fibrosis might be less relevant, as the endogenous gene is already downregulated. To examine the relevance of TCF21 downregulation with fibroblast activation, a mouse model was generated in which the human *TCF21* cDNA was inserted into the widely used noncoding portion of the *Col1a1* locus ≈500 base pairs downstream of the 3' untranslated region[26] (*Col1a1-TCF21* mice). As previously described,[27,28] the targeting construct was flanked by 2 mutant loxP sites, which resulted in the inversion of the DNA construct with Cre recombinase, thereby allowing expression of TCF21 (Figure 3A and 3B; see Methods section for details). As shown in Figure 3B, CFs isolated from the hearts of *Col1a1-TCF21*

mice and infected with an adenovirus-encoding Cre recombinase showed greater *TCF21* mRNA expression compared with beta-galactosidase–infected *Col1a1-TCF21* controls. It should be noted that due to sequence homology between mouse and human *TCF21*, the qRT-PCR primers likely amplified native mouse *Tcf21*.

Next, *Col1a1-TCF21* mice were crossed with a *Pdgfra-CreERT2* line to generate mice with tamoxifen induced TCF21 overexpression in CFs. *Pdgfra-CreERT2* or *Col1a1-TCF21* mice were used as controls. To permit the tracing of CFs after recombination, mice were further crossed with *Rosa26-loxP-STOP-loxP-eGFP* reporter mice. Adult mice were studied 1 week after tamoxifen injection (Figure 3C). PCR analysis of DNA isolated from hearts demonstrated successful inversion of the construct in *Pdgfra-CreERT2:Col1a1-TCF21* mice (Figure 3D). *Pdgfra-CreERT2* mice were used as controls. Immunofluorescence analysis from histological sections confirmed the coexpression of TCF21 protein (red) and eGFP in CFs from *Pdgfra-CreERT2:Col1a1-TCF21* mice compared with the lower detectable expression of endogenous TCF21 in *Pdgfra-CreERT2* control hearts (Figure 3E). qRT-PCR analysis of FAC-sorted eGFP+ CFs isolated 3 weeks after tamoxifen injection confirmed a robust induction of TCF21 mRNA in *Pdgfra-CreERT2:Col1a1-TCF21* cells compared with

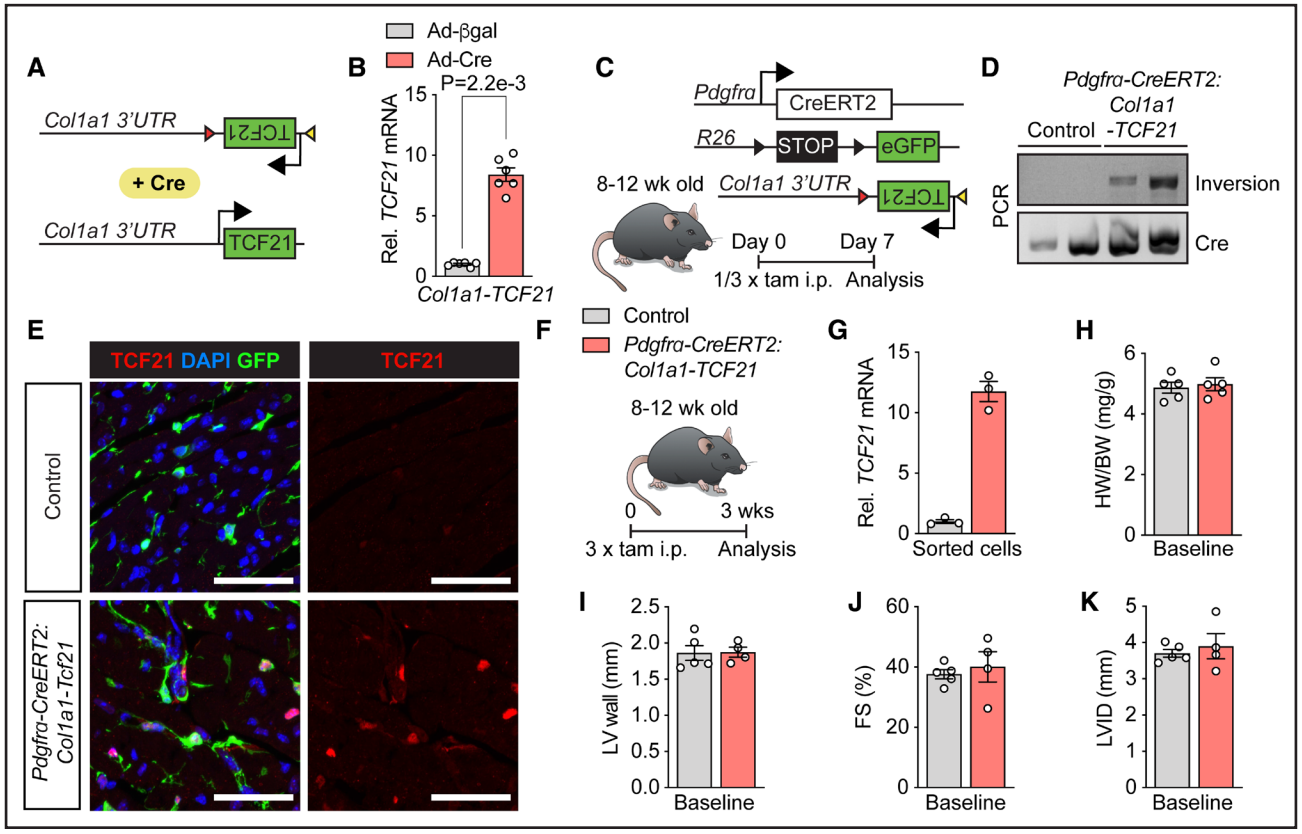

Figure 3. Generation of tamoxifen-inducible fibroblast-specific mice with enforced *TCF21* (transcription factor 21) expression. **A**, Schematic of the clustered regularly interspaced short palindromic repeats (CRISPR)-Cas9 modified mouse *Col1a1* genetic locus with inverted locus of crossover in P1 (loxP) sites and the human *TCF21* cDNA in the reverse direction, which, upon Cre-mediated recombination, gives proper orientation for gene expression. **B**, Quantitative real-time PCR (qRT-PCR) mRNA analysis for *TCF21* expression in cultured adult murine cardiac fibroblasts (CFs) infected with Ad-βgal (adenovirus-encoding beta-galactosidase) or Ad-Cre (adenovirus-encoding Cre recombinase). Data were normalized to *GAPDH* mRNA. **C**, Experimental schematic of crossed mice with the engineered *Col1a1-TCF21* allele, the *Rosa26-eGFP* conditional reporter allele, and the *Pdgfra-CreERT2* allele with the temporal experimental outline at the bottom. Tamoxifen (tam) was administered to 8- to 12-week-old mice for 1 or 3 consecutive days by intraperitoneal injection (i.p.) and harvested 7 days later. **D**, PCR analysis of Cre presence and DNA inversion of the *TCF21* cassette within the modified *Col1a1* locus upon Cre-mediated recombination in hearts from tam-treated mice as shown in **C**. *Pdgfra-CreERT2* mice were used as controls. **E**, Immunofluorescent images from heart histological sections of the 2 indicated groups of mice for TCF21 (red), recombined CFs (eGFP+ [enhanced green fluorescent protein]; green), and nuclei (blue; 4′,6-diamidino-2-phenylindole [DAPI] staining). The left 2 figures show all 3 channels, while the right 2 figures show only TCF21 antibody reactivity (red). Scale bars, 20 μm. **F**, Experimental scheme. Tam was administered by i.p. injection on 3 consecutive days to 8- to 12-week-old *Pdgfra-CreERT2:Col1a1-TCF21* mice and either *Pdgfra-CreERT2* or *Col1a1-TCF21* control mice and analyzed 3 weeks later. **G**, qRT-PCR analysis for *TCF21* cDNA expression from eGFP+ CFs isolated by fluorescence-activated cell sorting from hearts of the 2 groups of mice shown. **H**, Heart weight to body weight (HW/BW) ratio in the 2 indicated groups of mice. **I**, Echocardiographic analysis of left ventricular (LV) wall thickness in diastole, (**J**) fractional shortening (FS) %, and (**K**) LV internal diameter in diastole in the 2 indicated groups of mice. All data shown are mean±SEM. Samples were analyzed by a Kolmogorov-Smirnov test (exact *P* values are shown; **B** and **H**–**K**). For cell culture experiments, each n value shown represents CFs from an independent animal. All data points in graphs represent biological replicates.

Pdgfra-CreERT2 controls (Figure 3F and 3G). Importantly, at homeostasis, echocardiography demonstrated no statistically significant differences in cardiac structure or function with enforced TCF21 expression compared with control mice (*Pdgfra-CreERT2* or *Col1a1-TCF21*; Figure 3H through 3K).

Enforced Expression of TCF21 Inhibits Myofibroblast Differentiation and Fibrosis

To examine the effects of maintained TCF21 expression in response to a fibrotic stimulus, *Pdgfra-CreERT2*:*Col1a1-TCF21* or *Pdgfra-CreERT2* control mice were treated with tamoxifen and exposed to 1 week of Ang II/phenylephrine infusion (Figure 4A). Immunoblot assessment of CFs demonstrated markedly higher TCF21 expression in the hearts of *Pdgfra-CreERT2*:*Col1a1-TCF21* mice, without detectable changes in total αSMA protein expression after 1 week of Ang II/phenylephrine (Figure 4B). Ang II/phenylephrine-induced cardiac hypertrophy in both cohorts of mice; however, a stronger induction was observed in the *Pdgfra-CreERT2* control group compared with mice with fibroblast-specific enforced TCF21 expression (Figure 4C and 4D). To assess tissue fibroblast activity and fibrosis after 1 week of Ang II/phenylephrine, multiple nonsequential (1 mm apart) heart histological sections (at least 4 per mouse) were analyzed for TCF21 protein (red), fibroblast-lineage tracing (eGFP+), and myofibroblast cell state by αSMA expression (white). While hearts from mice with enforced TCF21 expression had regions of fibroblast accumulation that typifies fibrosis of this organ, they were largely devoid of αSMA expression in stress fibers compared with control *Pdgfra-CreERT2* hearts (Figure 4E). The deposition of collagen was assessed in the hearts by Sirius red histological staining, which demonstrated a significant induction of fibrosis by Ang II/phenylephrine in control mice but not in mice with enforced TCF21 expression in fibroblasts (Figure 4F and 4G; Figure S6). In response to Ang II/phenylephrine, deposition of the matricellular protein, POSTN (periostin), was readily detected within fibrotic regions of the heart by immunofluorescence staining (red) in *Pdgfra-CreERT2* control mice. In contrast, cardiac POSTN expression was largely absent in mice with enforced TCF21 expression (Figure 4H).

ECM and Fibrosis-Associated Genes Are Reduced in Fibroblasts With Enforced TCF21 Expression

To further investigate the mechanism, whereby enforced TCF21 expression impacts ECM deposition and fibroblast differentiation in vivo, bulk transcriptomic sequencing was performed on FAC-sorted eGFP+ CFs from hearts of *Pdgfra-CreERT2*:*Col1a1-TCF21* and *Pdgfra-CreERT2* control mice after 1 week of Ang II/phenylephrine stimulation (Figure 5A). This analysis identified 399 downregulated (log_2-FC >−1; false discovery rate <0.1) and 308 upregulated genes (log_2-FC >1; false discovery rate <0.1) that were differentially expressed (Figure 5A; Table S3). Gene ontology analysis of the downregulated genes in *Pdgfra-CreERT2*:*Col1a1-TCF21* CFs identified a substantial number of genes associated with ECM organization (Figure 5B; Table S3). Furthermore, numerous genes that characterize fibroblast activation and differentiation were reduced in CFs with enforced TCF21 expression (Figure 5C). To determine whether the observed downregulation of these genes was due to a lack of inducibility in response to Ang II/phenylephrine in CFs with enforced TCF21 expression, differential gene expression analysis was performed using data sets from CFs isolated from uninjured *Tcf21*^{MCM} hearts as the control condition (from Figure 1H). Principle component analysis demonstrated unique occupancies within the transcriptional space between the groups (Figure S7A). As expected, key fibrotic genes were upregulated by Ang II/phenylephrine in *Pdgfra-CreERT2* CFs when TCF21 expression is normally downregulated yet failed to be induced when TCF21 expression was maintained (Figure S7B). To validate the RNA-seq data set, eGFP+ CFs were sorted from a larger cohort of animals, and qRT-PCR analysis of selected fibrotic genes (*Fmod*, *Cthrc1*, *Itga11*, and *Comp*) was analyzed, which validated the bioinformatic data (Figure 5D through 5G). The expression of the ECM protein, COMP (cartilage oligomeric matrix protein), was of particular interest as it is critical for collagen secretion and assembly.[29] *Comp* was consistently suppressed by enforced TCF21 expression (Figure 5F). COMP protein (shown in red) was readily detectable in the hearts of control mice after fibrotic stimulation with Ang II/phenylephrine but was largely absent in the mice with enforced expression of TCF21 (Figure 5H).

Enforced Expression of TCF21 Promotes the Expression of Cell Cycle Genes

Gene ontology analysis of the upregulated genes by enforced TCF21 expression in CFs identified multiple pathways associated with the cell cycle (Figure S7C). qRT-PCR analysis of Ccnd1 (cyclin D1), which was identified as upregulated by RNA-sequencing analysis, was confirmed as significantly greater with enforced TCF21 expression in CFs compared with controls after Ang II/phenylephrine exposure in vivo (Figure S7D). To determine whether enforced TCF21 expression resulted in more fibroblasts in the heart after fibrotic stimulation, the experiment was repeated and eGFP+ CFs in the LV were quantified using flow cytometry 1 week after tamoxifen injection. While there were several *Pdgfra-CreERT2*:*Col1a1-TCF21* mice with more CFs than the *Pdgfra-CreERT2* control mice, the difference in eGFP+

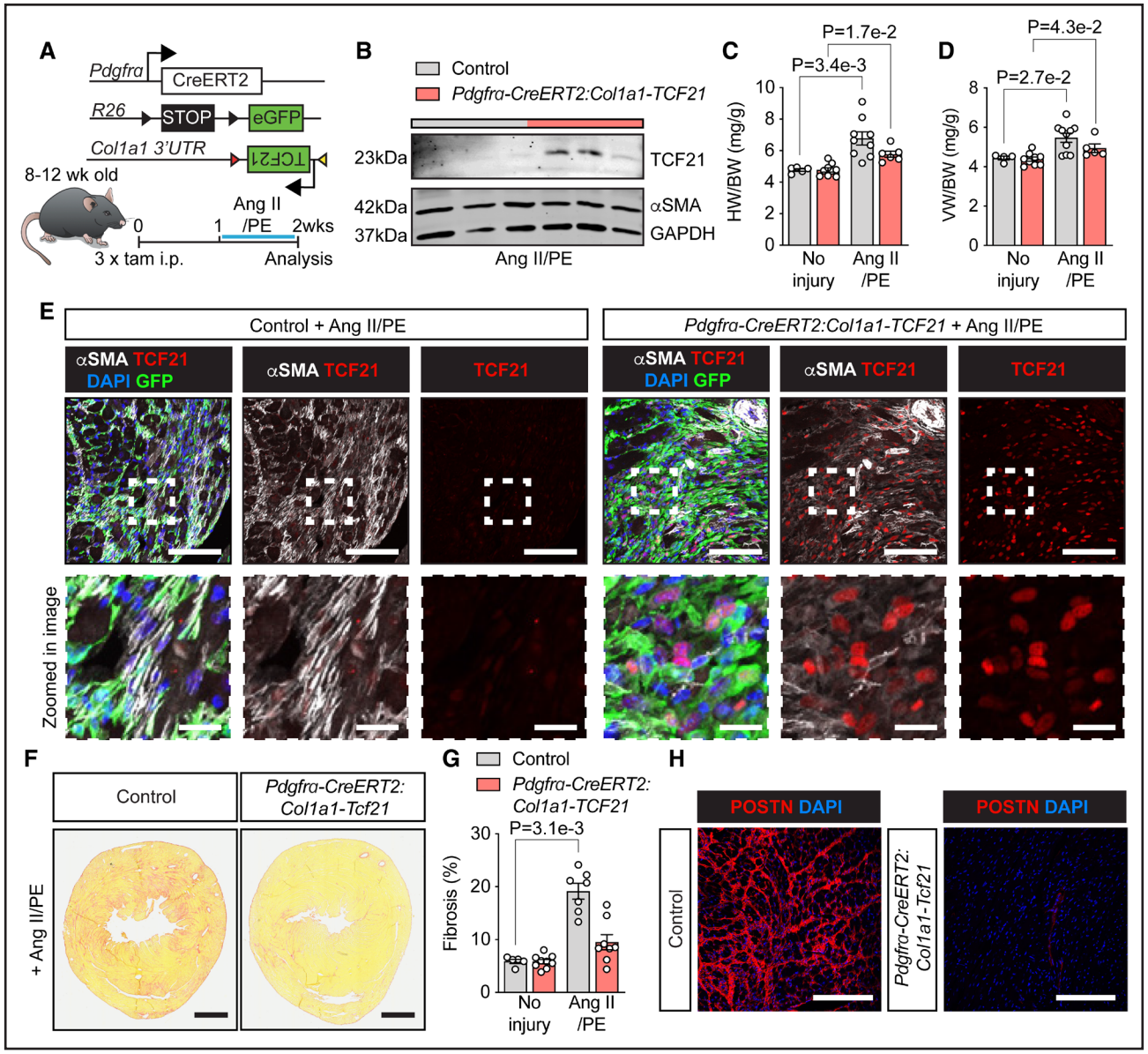

Figure 4. Cardiac fibroblast-specific enforced expression of TCF21 (transcription factor 21) reduces cardiac fibrosis.
A, Schematic of the genetically modified mouse alleles used and temporal experimental outline. This cross also contained the *Rosa26-eGFP* (enhanced green fluorescent protein) conditional reporter allele to show labeling within recombined fibroblasts. *Pdgfra-CreERT2* mice were used as controls. Tamoxifen (tam) was administered to 8- to 12-week-old mice for 3 consecutive days, followed by 1 week of Ang II (angiotensin II)/phenylephrine (PE) stimulation before analysis. **B**, Immunoblot analysis of TCF21 and αSMA (smooth muscle α-actin) protein expression in the 2 indicated groups of mice with Ang II/PE treatment as shown in **A** in cardiac fibroblasts (CFs) isolated by magnetic bead sorting with an anti-feeder cells antibody (clone mouse embryonic feeder cells [mEF-SK4]). Thirty micrograms of protein were loaded, and GAPDH was used as a loading/normalization control. **C**, Heart weight/body weight (HW/BW) ratio and (**D**) ventricular weight to BW ratio (VW/BW) ratio in the indicated groups of mice. **E**, Immunofluorescent histological images from hearts of the 2 indicated groups of mice with Ang II/PE stimulation stained for αSMA (white) and TCF21 (red) expression. Blue staining with 4′,6-diamidino-2-phenylindole (DAPI) shows nuclei, while green staining is eGFP expression in CFs due to recombination of the *Rosa26-eGFP* reporter allele. Scale bars, 50 μm. The lower row of images is a higher magnification of the boxed area in the upper images. Scale bars, 10 μm. **F**, Representative whole heart histological sections stained with Sirius red for collagen deposition from the 2 groups of mice shown with Ang II/PE stimulation. Scale bars, 1 mm. **G**, Quantification of percentage area of tissue fibrosis as shown in **F**. **H**, Immunofluorescent images from heart histological sections of *Pdgfra-CreERT2* control vs *Pdgfra-CreERT2:Col1a1-TCF21* mice for expression of POSTN (periostin, red) after 1 week of Ang II/PE. Nuclei are shown in blue with 4′,6-diamidino-2-phenylindole (DAPI) staining. Scale bars, 200 μm. All data shown are mean±SEM. Samples were analyzed by a Scheirer-Ray-Hare test with a Dunn post hoc test and the Benjamini Hochberg method for multiple test correction (exact adjusted *P* values are shown; **C**, **D**, and **G**). All data points in graphs represent biological replicates.

CFs between conditions did not reach statistical significance at this time point (Figure S7E). Taken together, our results demonstrate that the downregulation of TCF21 in CFs that occur in response to an injury is required for the differentiation of these cells into myofibroblasts and the development of fibrosis.

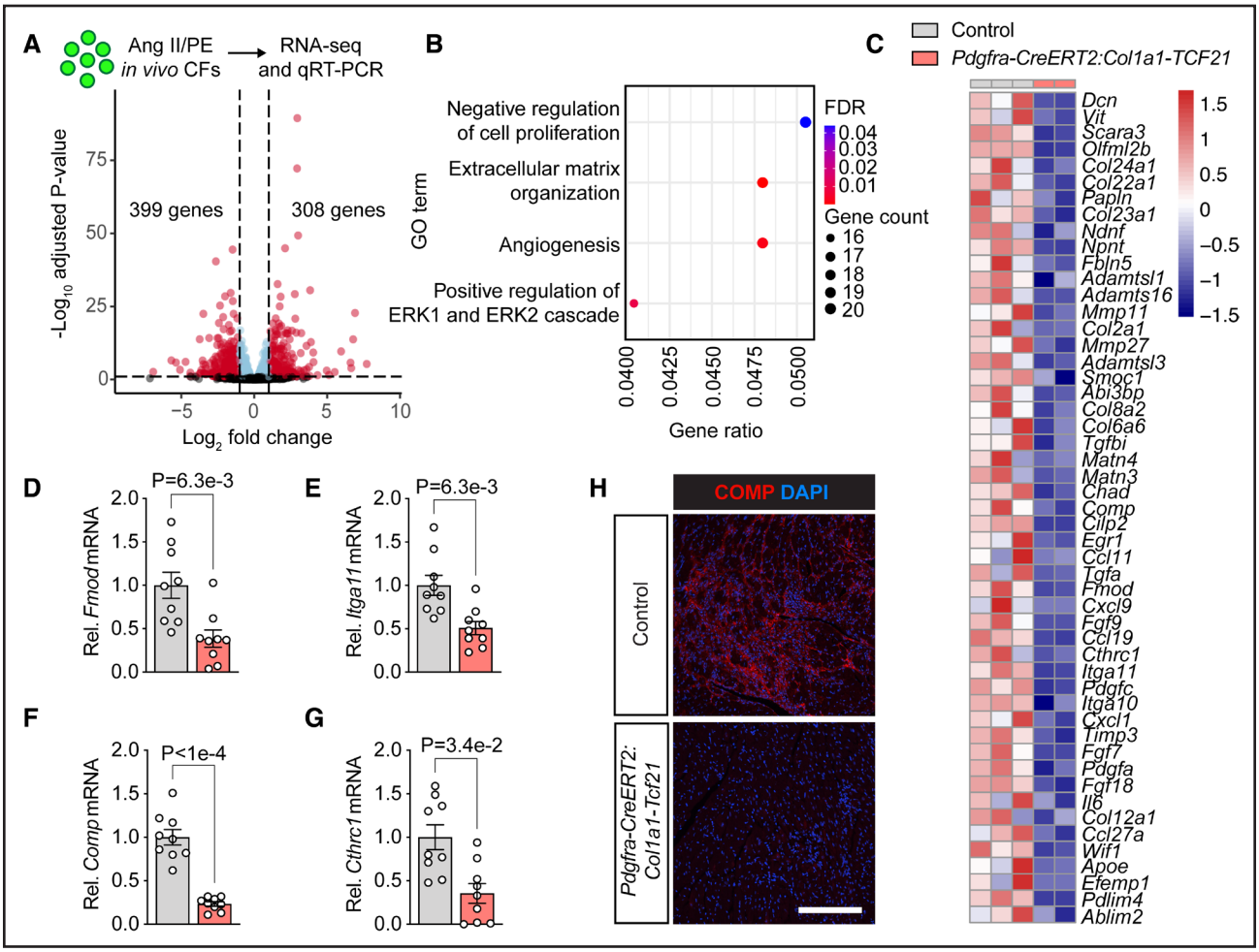

Figure 5. Cardiac fibroblast-specific enforced expression of TCF21 (transcription factor 21) reduces the expression of fibrosis genes.

A, Volcano plot of differentially expressed genes detected by bulk transcriptomic sequencing of eGFP+ (enhanced green fluorescent protein) cardiac fibroblasts (CFs) isolated by fluorescence-activated cell sorting (FACS) from hearts of *Pdgfra-CreERT2:Col1a1-TCF21* vs *Pdgfra-CreERT2* controls subject to 1 week of Ang II (angiotensin II)/phenylephrine (PE) stimulation. **B**, Dot plot of top gene ontology (GO) terms of biological processes with a false discovery rate (FDR) <0.05 of all downregulated genes with a log2-fold change (FC) >—1; FDR <0.1. The gene ratio is the proportion of genes that are present within the GO category. **C**, Heatmap of select Z-score normalized downregulated genes associated with fibroblast differentiation and fibrosis function from hearts of the 2 groups of mice shown with 1 week of Ang II/PE stimulation. The legend above **C** corresponds to the 3 and 2 samples shown by color above the heatmap. **D** through **G**, Quantitative real-time PCR (qRT-PCR) validation of select genes in eGFP+ CFs isolated by FACS of the 2 groups of mice after Ang II/PE. **H**, Immunofluorescent histological images from the hearts of *Pdgfra-CreERT2:Col1a1-TCF21* vs *Pdgfra-CreERT2* control mice following 1 week of Ang II/PE stimulation, stained with antibody against COMP (cartilage oligomeric matrix protein). Nuclei are shown in blue with 4′,6-diamidino-2-phenylindole (DAPI) staining. Scale bar, 200 µm. All data shown are mean±SEM. Samples were analyzed by a Kolmogorov-Smirnov test (exact *P* values are shown; **D**–**G**). All data points in graphs represent biological replicates.

Genome-Wide Occupancy Studies Identify TCF21 Binding in Genes Relevant to Cardiac Fibrosis

To further understand the regulatory role of TCF21, chromatin immunoprecipitation followed by sequencing was performed on CFs isolated and cultured from *Col1a1-TCF21* mice. TCF21 expression was induced with an adenovirus-encoding Cre recombinase, and cells were expanded for an additional 5 days. Transforming growth factor β, a potent inducer of fibroblast activation and differentiation to myofibroblasts, was added in the last 24 hours before chromatin immunoprecipitation and sequencing analysis. Motif enrichment analysis identified distinct TCF21 binding sites (CAGCTG) within peaks, validating the chromatin immunoprecipitation-seq data set (Figure 6A). A total of 19 614 binding sites were observed with a false discovery rate set at 0.001. These binding sites were distributed as follows: 6% were found within exons, 27% in intergenic regions, 41% within introns, 14% in promoters, and 12% in upstream regions (Figure 6B). TCF21 binding was present within genomic loci assigned to genes associated with fibroblast differentiation and fibrosis, including *Sox9*, *Acta2*,

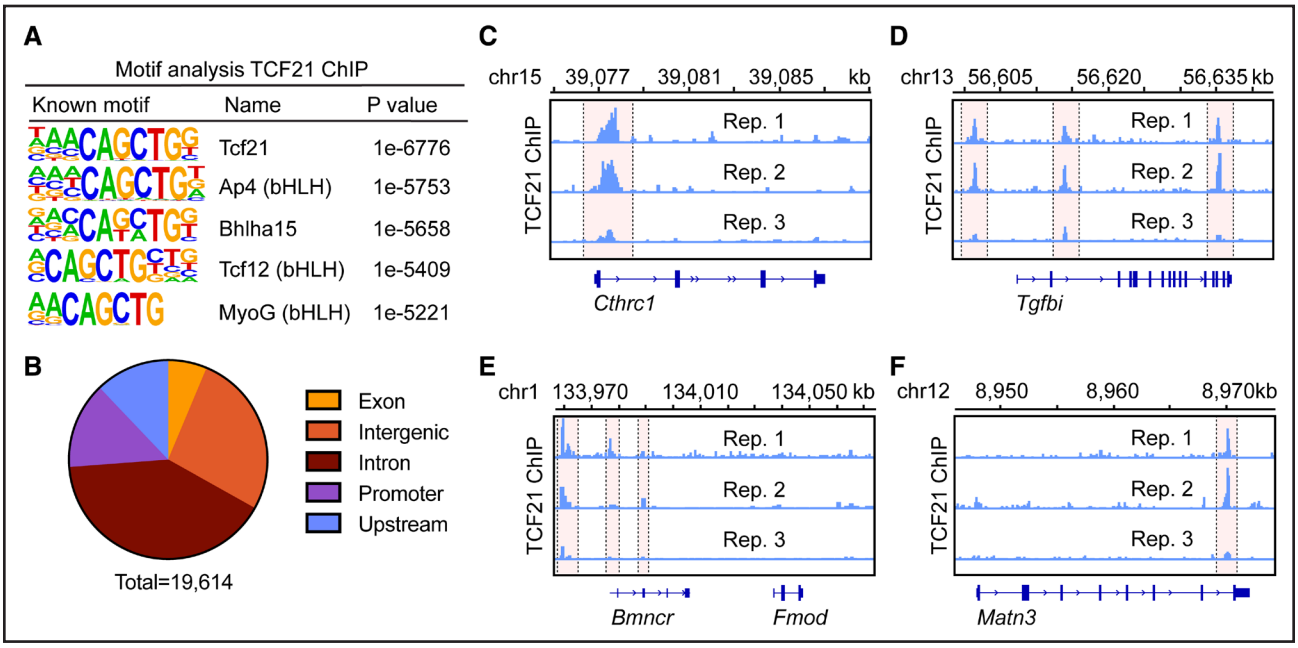

Figure 6. TCF21 (transcription factor 21) binds to genomic regions associated with cardiac fibroblast activation and fibrosis. **A**, Hypergeometric optimization of motif enrichment (HOMER) analysis of DNA sequence binding motifs in TCF21 chromatin immunoprecipitation (ChIP)-seq peaks in cultured cardiac myofibroblasts with enforced TCF21 expression. *Col1a1-TCF21* fibroblasts were infected with an Ad-Cre (adenovirus-encoding Cre recombinase) to induce TCF21 expression and expanded for 5 days. Transforming growth factor β (10 ng/mL) was added for the last 24 hours to induce myofibroblast differentiation. **B**, Pie chart showing peak distribution of annotated peaks. **C** through **F**, ChIP-seq peaks of select genes that are transcriptionally downregulated by TCF21. Each row represents a biological replicate (rep) that was derived from cardiac fibroblasts from 3 independent male and female mice. Ap4 indicates activator protein 4; bHLH, basic helix-loop-helix; Bhlha15, bHLH family member a15; and MyoG, myogenin.

Col1a1, *Col1a2*, and *Cthrc1* (Table S4; Figure 6C). Cross-referencing with genes that were identified as significantly downregulated by enforced TCF21 expression in CFs from mice treated with a continuous infusion of Ang II/phenylephrine (Figure 5C) identified numerous peaks in genomic loci, including *Cthrc1*, *Fmod*, *Matn3*, and *Tgfbi* (Figure 6D through 6F). While it is hypothesized that TCF21 exerts a repressive effect on gene expression,[6,9] distinct peaks were also identified in genes that were upregulated by enforced TCF21 expression (Table S3).

DISCUSSION

Deletion of the *Tcf21* gene from adult CFs did not alter how these cells function at homeostasis, nor did it affect their ability to promote cardiac fibrosis after myocardial injury. While, initially, this result was unanticipated, it aligns with previous observations in acute cardiac injury, whereby TCF21 expression in newly activated fibroblasts becomes downregulated. Hence, it is not surprising that deleting this gene from a cell type that already transcriptionally represses *Tcf21* expression during differentiation into a myofibroblast state[3–5] did not have a notable effect. While subtle, significant changes in mRNA expression of a subset of genes associated with the myofibroblast state were detected upon baseline deletion of *Tcf21* in vivo, it failed to translate into a phenotype. However, it remains possible that fibroblast-specific deletion of *Tcf21* in mice with advanced aging or chronic cardiomyopathies might eventually demonstrate a discernible effect.

In contrast, maintaining TCF21 expression in CFs during stimulation with Ang II/phenylephrine, when it would normally be downregulated, inhibited the proper differentiation of these cells into myofibroblasts with αSMA-expressing stress fibers, leading to a significant reduction in total heart fibrosis. The allele driving TCF21 expression was inserted into the 3' untranslated region of the *Col1a1* gene, and this strategy is often used to generate physiological levels of expression for interrogating gene function. Mechanistically, we hypothesize that TCF21 functions as a repressor of fibroblast activation and differentiation toward the myofibroblast fate. Indeed, key genes associated with the myofibroblast and cardiac fibrosis, such as *Cthrc1*,[30] *Pdgfa*,[31] and *Itga11*,[32] failed to be induced after fibrotic agonist stimulation in vivo when TCF21 expression was maintained. Moreover, genes previously associated with matrifibrocytes and the formation of a mature stable scar, *Chad*, *Comp*, and *Cilp2*,[3] were robustly induced by Ang II/phenylephrine in control fibroblasts yet failed to be induced when TCF21 expression was maintained. *Comp* is a noncollagenous matricellular protein that is upregulated in tissues with keloids, scleroderma, systemic sclerosis,[33] pulmonary fibrosis,[34] and ischemic heart disease.[3] In a larger cohort

of mice treated with Ang II/phenylephrine, *Comp* mRNA expression was found to be consistently downregulated in fibroblasts when TCF21 expression was maintained. In response to pathological insults, such as Ang II/phenylephrine, CFs induce the expression of POSTN.[35] POSTN is involved in collagen fibrillogenesis, directly binding to type I collagen, and is found in collagen-rich tissues that are exposed to high mechanical tension.[36] Although no differences in *Postn* mRNA levels were detected after 1 week of Ang II/phenylephrine treatment with enforced *TCF21* expression, the reduced induction of fibrosis may have prevented the deposition of POSTN protein within the ECM, as observed. Alternatively, we may simply have missed the window of maximal POSTN mRNA induction in control hearts with Ang II/phenylephrine. Genome-wide occupancy studies identified *Tcf21* binding in key genes associated with the myofibroblast, fibrosis, and the ECM, including *Sox9*, *Acta2*, *Col1a1*, *Col1a2*, *Cthrc1*, *Fmod*, *Matn3*, and *Tgfbi*, further supporting a role for TCF21 in regulating the ECM. While not all these genes were differentially expressed by enforced TCF21 expression after 1 week of Ang II/phenylephrine, it is plausible that altered expression may be observed at different time points.

Enforced expression of TCF21 also upregulated the expression of genes associated with the cell cycle after fibrotic stimulation although no significant changes in CF cell numbers were detected at the same time point. Cell cycle activity is enhanced in fibroblasts in response to injury, which is reduced as fibroblasts differentiate toward myofibroblasts.[3] Thus, the induction in cell cycle genes could be a direct effect of TCF21 expression or secondary to reduced differentiation to myofibroblasts. Future studies will assess whether sustained TCF21 expression with aging affects total CF cell numbers in the uninjured heart or how fibrosis and CF activities are affected in chronic cardiomyopathies.

In smooth muscle cells, TCF21 promotes the expression of proinflammatory genes by interaction with other bHLH transcription factors.[37] Although deletion or enforced TCF21 expression in CFs did not result in a profound inflammatory profile, a slight, yet significantly greater cardiac neutrophil content was present after fibroblast loss of *Tcf21*. While these neutrophils are likely quiescent in the absence of tissue injury,[38] it demonstrates a potential role for TCF21 in regulating cytokine or chemokine gene expression in fibroblasts. Indeed, CFs were recently shown to directly regulate the immune response in the heart through expression of major histocompatibility complex class II genes and antigen presentation to T-cells, which was necessary for the development of fibrosis.[39]

In conclusion, these studies demonstrate that the loss of *Tcf21* in CFs is necessary for the development of cardiac fibrosis. We recognize that the small sample sizes utilized, particularly in RNA sequencing experiments and some disease models, may result in an increased false positive rate and may underpower the ability to detect true effects. Future studies will aim to determine the cofactors of TCF21 and to define its regulatory function of gene expression of tissue-resident fibroblasts and how they are regulated during disease.

ARTICLE INFORMATION

Received September 10, 2024; revision received November 7, 2024; accepted November 24, 2024.

Affiliations

Division of Molecular Cardiovascular Biology (A.K.Z.J., R.K.K., R.J.V., S.-C.J.L., S.L.K.B., Y.K., K.M.G., K.W., M.A.S., T.A.B., J.D.M.), Division of Pulmonary and Critical Care Medicine (J.G.-A.), Division of Allergy and Immunology (A.S., A.B.), and Division of Human Genetics (A.S., A.B.), Department of Pediatrics, University of Cincinnati and Cincinnati Children's Hospital Medical Center, OH. Division of Cardiology, Department of Medicine, Consortium for Fibrosis Research and Translation, University of Colorado Anschutz Medical Campus, Aurora (R.J.V.). Feinberg Cardiovascular Research and Renal Institute, Deptartment of Medicine, Northwestern University, Chicago, IL (S.E.O.).

Acknowledgments

This research was made possible by, in part, using the Cincinnati Children's Shared Research Flow Cytometry Facility, the Veterinary Services Facility, the Single Cell Genomics Facility, the Transgenic Animal and Genome Editing Facility, the Integrated Pathology Research Facility, and the Bio-Imaging and Analysis Facility. The graphical abstract was created in BioRender: Johansen, A. (2024) BioRender.com/m95m314.

Author Contributions

A.K.Z. Johansen and J.D. Molkentin conceptualized, designed, performed, and analyzed the experiments and wrote the article. R.K. Kasam, R.J. Vagnozzi, and T.A. Baldwin performed and analyzed experiments. J.G. Gomez-Arroyo designed and analyzed experiments. A. Shittu designed, performed, and analyzed experiments. S.K.L. Bowers, Y. Kuwabara, K.M. Grimes, K. Warrick, S.-C.J. Lin, and M.A. Sargent performed experiments. A. Barski designed experiments and provided critical input. S.E. Quaggin provided reagents and critical input. All authors reviewed and provided comments on the article.

Sources of Funding

This work was supported by grants from the National Institutes of Health (R01HL142217 and R01HL160765 to J.D. Molkentin, STTR R42HG011219 to Datirium, and R01AI153442 to A. Barski).

Disclosures

A. Barski is a co-founder of Datirium, LLC, the developer of the Scientific Data Analysis Platform (https://scidap.com) used here to analyze chromatin immunoprecipitation followed by sequencing data.

Supplemental Material

Supplemental Methods
Tables S1–S4
Figures S1–S7
Major Resources Table
References 40–56

REFERENCES

1. Acharya A, Baek ST, Huang G, Eskiocak B, Goetsch S, Sung CY, Banfi S, Sauer MF, Olsen GS, Duffield JS, et al. The bHLH transcription factor Tcf21 is required for lineage-specific EMT of cardiac fibroblast progenitors. *Development.* 2012;139:2139–2149. doi: 10.1242/dev.079970
2. Lu J, Richardson JA, Olson EN. Capsulin: a novel bHLH transcription factor expressed in epicardial progenitors and mesenchyme of visceral organs. *Mech Dev.* 1998;73:23–32. doi: 10.1016/s0925-4773(98)00030-6
3. Fu X, Khalil H, Kanisicak O, Boyer JG, Vagnozzi RJ, Maliken BD, Sargent MA, Prasad V, Valiente-Alandi I, Blaxall BC, et al. Specialized fibroblast differentiated states underlie scar formation in the infarcted mouse heart. *J Clin Invest.* 2018;128:2127–2143. doi: 10.1172/JCI98215

4. Liu X, Burke RM, Lighthouse JK, Baker CD, Dirkx RA Jr, Kang B, Chakraborty Y, Mickelsen DM, Twardowski JJ, Mello SS, et al. p53 Regulates the extent of fibroblast proliferation and fibrosis in left ventricle pressure overload. *Circ Res*. 2023;133:271–287. doi: 10.1161/CIRCRESAHA.121.320324
5. Kanisicak O, Khalil H, Ivey MJ, Karch J, Maliken BD, Correll RN, Brody MJ, SC JL, Aronow BJ, Tallquist MD, et al. Genetic lineage tracing defines myofibroblast origin and function in the injured heart. *Nat Commun*. 2016;7:12260. doi: 10.1038/ncomms12260
6. Nurnberg ST, Cheng K, Raiesdana A, Kundu R, Miller CL, Kim JB, Arora K, Carcamo-Oribe I, Xiong Y, Tellakula N, et al. Coronary artery disease associated transcription factor TCF21 regulates smooth muscle precursor cells that contribute to the fibrous cap. *PLoS Genet*. 2015;11:e1005155. doi: 10.1371/journal.pgen.1005155
7. Skalli O, Ropraz P, Trzeciak A, Benzonana G, Gillessen D, Gabbiani G. A monoclonal antibody against alpha-smooth muscle actin: a new probe for smooth muscle differentiation. *J Cell Biol*. 1986;103:2787–2796. doi: 10.1083/jcb.103.6.2787
8. Muhl L, Genove G, Leptidis S, Liu J, He L, Mocci G, Sun Y, Gustafsson S, Buyandelger B, Chivukula IV, et al. Single-cell analysis uncovers fibroblast heterogeneity and criteria for fibroblast and mural cell identification and discrimination. *Nat Commun*. 2020;11:3953. doi: 10.1038/s41467-020-17740-1
9. Sazonova O, Zhao Y, Nurnberg S, Miller C, Pjanic M, Castano VG, Kim JB, Salfati EL, Kundaje AB, Bejerano G, et al. Characterization of TCF21 downstream target regions identifies a transcriptional network linking multiple independent coronary artery disease loci. *PLoS Genet*. 2015;11:e1005202. doi: 10.1371/journal.pgen.1005202
10. Eijgenraam TR, Sillje HHW, de Boer RA. Current understanding of fibrosis in genetic cardiomyopathies. *Trends Cardiovasc Med*. 2020;30:353–361. doi: 10.1016/j.tcm.2019.09.003
11. Gulati A, Jabbour A, Ismail TF, Guha K, Khwaja J, Raza S, Morarji K, Brown TD, Ismail NA, Dweck MR, et al. Association of fibrosis with mortality and sudden cardiac death in patients with nonischemic dilated cardiomyopathy. *JAMA*. 2013;309:896–908. doi: 10.1001/jama.2013.1363
12. Plikus MV, Wang X, Sinha S, Forte E, Thompson SM, Herzog EL, Driskell RR, Rosenthal N, Biernaskie J, Horsley V. Fibroblasts: Origins, definitions, and functions in health and disease. *Cell*. 2021;184:3852–3872. doi: 10.1016/j.cell.2021.06.024
13. Khalil H, Kanisicak O, Prasad V, Correll RN, Fu X, Schips T, Vagnozzi RJ, Liu R, Huynh T, Lee SJ, et al. Fibroblast-specific TGF-beta-Smad2/3 signaling underlies cardiac fibrosis. *J Clin Invest*. 2017;127:3770–3783. doi: 10.1172/JCI94753
14. Kuwabara JT, Hara A, Bhutada S, Gojanovich GS, Chen J, Hokutan K, Shettigar V, Lee AY, DeAngelo LP, Heckl JR, et al. Consequences of PDGFRalpha$^+$ fibroblast reduction in adult murine hearts. *Elife*. 2022;11:e69854. doi: 10.7554/eLife.69854
15. Garoffolo G, Casaburo M, Amadeo F, Salvi M, Bernava G, Piacentini L, Chimenti I, Zaccagnini G, Milcovich G, Zuccolo E, et al. Reduction of cardiac fibrosis by interference with YAP-dependent transactivation. *Circ Res*. 2022;131:239–257. doi: 10.1161/CIRCRESAHA.121.319373
16. Maezawa Y, Onay T, Scott RP, Keir LS, Dimke H, Li C, Eremina V, Maezawa Y, Jeansson M, Shan J, et al. Loss of the podocyte-expressed transcription factor Tcf21/Pod1 results in podocyte differentiation defects and FSGS. *J Am Soc Nephrol*. 2014;25:2459–2470. doi: 10.1681/ASN.2013121307
17. Quaggin SE, Schwartz L, Cui S, Igarashi P, Deimling J, Post M, Rossant J. The basic-helix-loop-helix protein pod1 is critically important for kidney and lung organogenesis. *Development*. 1999;126:5771–5783. doi: 10.1242/dev.126.24.5771
18. Lu J, Chang P, Richardson JA, Gan L, Weiler H, Olson EN. The basic helix-loop-helix transcription factor capsulin controls spleen organogenesis. *Proc Natl Acad Sci USA*. 2000;97:9525–9530. doi: 10.1073/pnas.97.17.9525
19. Acharya A, Baek ST, Banfi S, Eskiocak B, Tallquist MD. Efficient inducible Cre-mediated recombination in Tcf21 cell lineages in the heart and kidney. *Genesis*. 2011;49:870–877. doi: 10.1002/dvg.20750
20. Chung MI, Bujnis M, Barkauskas CE, Kobayashi Y, Hogan BLM. Niche-mediated BMP/SMAD signaling regulates lung alveolar stem cell proliferation and differentiation. *Development*. 2018;145:dev163014. doi: 10.1242/dev.163014
21. Ivey MJ, Kuwabara JT, Pai JT, Moore RE, Sun Z, Tallquist MD. Resident fibroblast expansion during cardiac growth and remodeling. *J Mol Cell Cardiol*. 2018;114:161–174. doi: 10.1016/j.yjmcc.2017.11.012
22. Moore-Morris T, Guimaraes-Camboa N, Banerjee I, Zambon AC, Kisseleva T, Velayoudon A, Stallcup WB, Gu Y, Dalton ND, Cedenilla M, et al. Resident fibroblast lineages mediate pressure overload-induced cardiac fibrosis. *J Clin Invest*. 2014;124:2921–2934. doi: 10.1172/JCI74783
23. Smith CL, Baek ST, Sung CY, Tallquist MD. Epicardial-derived cell epithelial-to-mesenchymal transition and fate specification require PDGF receptor signaling. *Circ Res*. 2011;108:e15–e26. doi: 10.1161/CIRCRESAHA.110.235531
24. Ao X, Ding W, Zhang Y, Ding D, Liu Y. TCF21: a critical transcription factor in health and cancer. *J Mol Med (Berl)*. 2020;98:1055–1068. doi: 10.1007/s00109-020-01934-7
25. Forte E, Skelly DA, Chen M, Daigle S, Morelli KA, Hon O, Philip VM, Costa MW, Rosenthal NA, Furtado MB. Dynamic interstitial cell response during myocardial infarction predicts resilience to rupture in genetically diverse mice. *Cell Rep*. 2020;30:3149–3163.e6. doi: 10.1016/j.celrep.2020.02.008
26. Beard C, Hochedlinger K, Plath K, Wutz A, Jaenisch R. Efficient method to generate single-copy transgenic mice by site-specific integration in embryonic stem cells. *Genesis*. 2006;44:23–28. doi: 10.1002/gene.20180
27. Huijbers IJ, Del Bravo J, Bin Ali R, Pritchard C, Braumuller TM, van Miltenburg MH, Henneman L, Michalak EM, Berns A, Jonkers J. Using the GEMM-ESC strategy to study gene function in mouse models. *Nat Protoc*. 2015;10:1755–1785. doi: 10.1038/nprot.2015.114
28. Zhang Z, Lutz B. Cre recombinase-mediated inversion using lox66 and lox71: method to introduce conditional point mutations into the CREB-binding protein. *Nucleic Acids Res*. 2002;30:e90. doi: 10.1093/nar/gnf089
29. Schulz JN, Nuchel J, Niehoff A, Bloch W, Schonborn K, Hayashi S, Kamper M, Brinckmann J, Plomann M, Paulsson M, et al. COMP-assisted collagen secretion--a novel intracellular function required for fibrosis. *J Cell Sci*. 2016;129:706–716. doi: 10.1242/jcs.180216
30. Ruiz-Villalba A, Romero JP, Hernandez SC, Vilas-Zornoza A, Fortelny N, Castro-Labrador L, San Martin-Uriz P, Lorenzo-Vivas E, Garcia-Olloqui P, Palacio M, et al. Single-cell RNA sequencing analysis reveals a crucial role for CTHRC1 (collagen triple helix repeat containing 1) cardiac fibroblasts after myocardial infarction. *Circulation*. 2020;142:1831–1847. doi: 10.1161/CIRCULATIONAHA.119.044557
31. Gallini R, Lindblom P, Bondjers C, Betsholtz C, Andrae J. PDGF-A and PDGF-B induces cardiac fibrosis in transgenic mice. *Exp Cell Res*. 2016;349:282–290. doi: 10.1016/j.yexcr.2016.10.022
32. Civitarese RA, Talior-Volodarsky I, Desjardins JF, Kabir G, Switzer J, Mitchell M, Kapus A, McCulloch CA, Gullberg D, Connelly KA. The alpha11 integrin mediates fibroblast-extracellular matrix-cardiomyocyte interactions in health and disease. *Am J Physiol Heart Circ Physiol*. 2016;311:H96–H106. doi: 10.1152/ajpheart.00918.2015
33. Agarwal P, Schulz JN, Blumbach K, Andreasson K, Heinegard D, Paulsson M, Mauch C, Eming SA, Eckes B, Krieg T. Enhanced deposition of cartilage oligomeric matrix protein is a common feature in fibrotic skin pathologies. *Matrix Biol*. 2013;32:325–331. doi: 10.1016/j.matbio.2013.02.010
34. Vuga LJ, Milosevic J, Pandit K, Ben-Yehudah A, Chu Y, Richards T, Sciurba J, Myerburg M, Zhang Y, Parwani AV, et al. Cartilage oligomeric matrix protein in idiopathic pulmonary fibrosis. *PLoS One*. 2013;8:e83120. doi: 10.1371/journal.pone.0083120
35. Snider P, Standley KN, Wang J, Azhar M, Doetschman T, Conway SJ. Origin of cardiac fibroblasts and the role of periostin. *Circ Res*. 2009;105:934–947. doi: 10.1161/CIRCRESAHA.109.201400
36. Norris RA, Damon B, Mironov V, Kasyanov V, Ramamurthi A, Moreno-Rodriguez R, Trusk T, Potts JD, Goodwin RL, Davis J, et al. Periostin regulates collagen fibrillogenesis and the biomechanical properties of connective tissues. *J Cell Biochem*. 2007;101:695–711. doi: 10.1002/jcb.21224
37. Kim JB, Pjanic M, Nguyen T, Miller CL, Iyer D, Liu B, Wang T, Sazonova O, Carcamo-Orive I, Matic LP, et al. TCF21 and the environmental sensor aryl-hydrocarbon receptor cooperate to activate a pro-inflammatory gene expression program in coronary artery smooth muscle cells. *PLoS Genet*. 2017;13:e1006750. doi: 10.1371/journal.pgen.1006750
38. Mayadas TN, Cullere X, Lowell CA. The multifaceted functions of neutrophils. *Annu Rev Pathol*. 2014;9:181–218. doi: 10.1146/annurev-pathol-020712-164023
39. Ngwenyama N, Kaur K, Bugg D, Theall B, Aronovitz M, Berland R, Panagiotidou S, Genco C, Perrin MA, Davis J, et al. Antigen presentation by cardiac fibroblasts promotes cardiac dysfunction. *Nat Cardiovasc Res*. 2022;1:761–774. doi: 10.1038/s44161-022-00116-7
40. Schwenk F, Baron U, Rajewsky K. A cre-transgenic mouse strain for the ubiquitous deletion of loxP-flanked gene segments including deletion in germ cells. *Nucleic Acids Res*. 1995;23:5080–5081. doi: 10.1093/nar/23.24.5080
41. Yamamoto M, Shook NA, Kanisicak O, Yamamoto S, Wosczyna MN, Camp JR, Goldhamer DJ. A multifunctional reporter mouse line for Cre- and FLP-dependent lineage analysis. *Genesis*. 2009;47:107–114. doi: 10.1002/dvg.20474

42. Bray NL, Pimentel H, Melsted P, Pachter L. Near-optimal probabilistic RNA-seq quantification. *Nat Biotechnol*. 2016;34:525–527. doi: 10.1038/nbt.3519
43. Soneson C, Love MI, Robinson MD. Differential analyses for RNA-seq: transcript-level estimates improve gene-level inferences. *F1000Res*. 2015;4:1521. doi: 10.12688/f1000research.7563.2
44. Love MI, Huber W, Anders S. Moderated estimation of fold change and dispersion for RNA-seq data with DESeq2. *Genome Biol*. 2014;15:550. doi: 10.1186/s13059-014-0550-8
45. Sherman BT, Hao M, Qiu J, Jiao X, Baseler MW, Lane HC, Imamichi T, Chang W. DAVID: a web server for functional enrichment analysis and functional annotation of gene lists (2021 update). *Nucleic Acids Res*. 2022;50:W216–W221. doi: 10.1093/nar/gkac194
46. Huang da W, Sherman BT, Lempicki RA. Systematic and integrative analysis of large gene lists using DAVID bioinformatics resources. *Nat Protoc*. 2009;4:44–57. doi: 10.1038/nprot.2008.211
47. Forte E, Daigle S, Rosenthal NA. Protocol for isolation of cardiac interstitial cells from adult murine hearts for unbiased single cell profiling. *STAR Protoc*. 2020;1:100077. doi: 10.1016/j.xpro.2020.100077
48. Hao Y, Hao S, Andersen-Nissen E, Mauck WM 3rd, Zheng S, Butler A, Lee MJ, Wilk AJ, Darby C, Zager M, et al. Integrated analysis of multimodal single-cell data. *Cell*. 2021;184:3573–3587.e29. doi: 10.1016/j.cell.2021.04.048
49. Yukawa M, Jagannathan S, Vallabh S, Kartashov AV, Chen X, Weirauch MT, Barski A. AP-1 activity induced by co-stimulation is required for chromatin opening during T cell activation. *J Exp Med*. 2020;217:e20182009. doi: 10.1084/jem.20182009
50. Schmidl C, Rendeiro AF, Sheffield NC, Bock C. ChIPmentation: fast, robust, low-input ChIP-seq for histones and transcription factors. *Nat Methods*. 2015;12:963–965. doi: 10.1038/nmeth.3542
51. Buenrostro JD, Giresi PG, Zaba LC, Chang HY, Greenleaf WJ. Transposition of native chromatin for fast and sensitive epigenomic profiling of open chromatin, DNA-binding proteins and nucleosome position. *Nat Methods*. 2013;10:1213–1218. doi: 10.1038/nmeth.2688
52. Langmead B, Salzberg SL. Fast gapped-read alignment with Bowtie 2. *Nat Methods*. 2012;9:357–359. doi: 10.1038/nmeth.1923
53. Zhang Y, Liu T, Meyer CA, Eeckhoute J, Johnson DS, Bernstein BE, Nusbaum C, Myers RM, Brown M, Li W, et al. Model-based analysis of ChIP-Seq (MACS). *Genome Biol*. 2008;9:R137. doi: 10.1186/gb-2008-9-9-r137
54. Quinlan AR, Hall IM. BEDTools: a flexible suite of utilities for comparing genomic features. *Bioinformatics*. 2010;26:841–842. doi: 10.1093/bioinformatics/btq033
55. Robinson JT, Thorvaldsdottir H, Winckler W, Guttman M, Lander ES, Getz G, Mesirov JP. Integrative genomics viewer. *Nat Biotechnol*. 2011;29:24–26. doi: 10.1038/nbt.1754
56. Heinz S, Benner C, Spann N, Bertolino E, Lin YC, Laslo P, Cheng JX, Murre C, Singh H, Glass CK. Simple combinations of lineage-determining transcription factors prime cis-regulatory elements required for macrophage and B cell identities. *Mol Cell*. 2010;38:576–589. doi: 10.1016/j.molcel.2010.05.004